Riboflavin transporter SLC52A1, a target of p53, suppresses cellular senescence by activating mitochondrial complex II

Nagano, Taiki ; Awai, Yuto ; Kuwaba, Shione ; Osumi, Taiichi ; Mio, Kentaro ; Iwasaki, Tetsushi ; Kamada, Shinji

(Citation)
Molecular Biology of the Cell,32(21)

(Issue Date)
2021-11-01

(Resource Type)
journal article

(Version)
Version of Record

Riboflavin transporter SLC52A1, a target of p53, suppresses cellular senescence by activating mitochondrial complex II

Taiki Nagano[a], Yuto Awai[b], Shione Kuwaba[b], Taiichi Osumi[c], Kentaro Mio[c], Tetsushi Iwasaki[a,b,c], and Shinji Kamada[a,b,c,*]

[a]Biosignal Research Center, [b]Department of Biology, Faculty of Science, and [c]Department of Biology, Graduate School of Science, Kobe University, Nada-ku, Kobe 657-8501, Japan

ABSTRACT **Cellular senescence is a state of permanent proliferative arrest induced by a variety of stresses, such as DNA damage. The transcriptional activity of p53 has been known to be essential for senescence induction. It remains unknown, however, whether among the downstream genes of p53, there is a gene that has antisenescence function. Our recent studies have indicated that the expression of SLC52A1 (also known as GPR172B/RFVT1), a riboflavin transporter, is up-regulated specifically in senescent cells depending on p53, but the relationship between senescence and SLC52A1 or riboflavin has not been described. Here, we examined the role of SLC52A1 in senescence. We found that knockdown of *SLC52A1* promoted senescence phenotypes induced by DNA damage in tumor and normal cells. The senescence suppressive action of SLC52A1 was dependent on its riboflavin transport activity. Furthermore, elevation of intracellular riboflavin led to activation of mitochondrial membrane potential (MMP) mediated by the mitochondrial electron transport chain complex II. Finally, the SLC52A1-dependent activation of MMP inhibited the AMPK-p53 pathway, a central mediator of mitochondria dysfunction–related senescence. These results suggest that SLC52A1 contributes to suppress senescence through the uptake of riboflavin and acts downstream of p53 as a negative feedback mechanism to limit aberrant senescence induction.**

Monitoring Editor
Jody Rosenblatt
King's College London

Received: May 25, 2021
Revised: Sep 3, 2021
Accepted: Sep 9, 2021

INTRODUCTION

SLC52A1 (also known as GPR172B/RFVT1) is a riboflavin transporter that is highly expressed in the placenta, small intestine, duodenum, etc. (Yonezawa and Inui, 2013; Fagerberg *et al.*, 2014). Riboflavin is a water-soluble vitamin also termed vitamin B_2, and in cells, it is metabolically converted to flavin mononucleotide and then to flavin adenine dinucleotide (FAD) by FAD synthetase (Powers, 2003). FAD is an intermediate in the electron transfer reactions of biological oxidation-reduction processes and hence functions as a coenzyme of many metabolic enzymes such as ones involved in the mitochondrial electron transport chain (ETC) and tricarboxylic acid cycle (Udhayabanu *et al.*, 2017). FAD in particular serves as a vital component of ETC-mediated ATP production required for normal cell growth and proper energy-dependent cellular functions (Spaan *et al.*, 2005; Ho *et al.*, 2011).

Recently, it is becoming clear that mitochondrial dysfunction promotes cellular senescence, a state of permanent growth arrest induced by various stresses such as DNA damage (Campisi 2013; Salama *et al.*, 2014; Wiley *et al.*, 2016; Abate *et al.*, 2020). Senescent cells can accumulate with age and be involved in age-related diseases through the depletion of proliferative stem cell pools and the secretion of proinflammatory cytokines. In response to DNA damage, cells activate a complex signaling cascade called the DNA damage response, which results in the activation of tumor suppressor p53, a transcriptional factor essential for the induction of senescence (Vousden and Prives, 2009; Rufini *et al.*, 2013). The activated p53 up-regulates the expression of a number of genes involved in senescence. Among these genes, several genes have been proven to promote senescence. For example, p21 has been recognized as a pivotal mediator of p53-dependent cell cycle arrest through

This article was published online ahead of print in MBoC in Press (http://www.molbiolcell.org/cgi/doi/10.1091/mbc.E21-05-0262) on September 15, 2021.

*Address correspondence to: Shinji Kamada (skamada@kobe-u.ac.jp).

Abbreviations used: ETC, electron transport chain; FAD, flavin adenine dinucleotide; MMP, mitochondrial membrane potential; qPCR, quantitative PCR; TTFA, thenoyltrifluoroacetone.

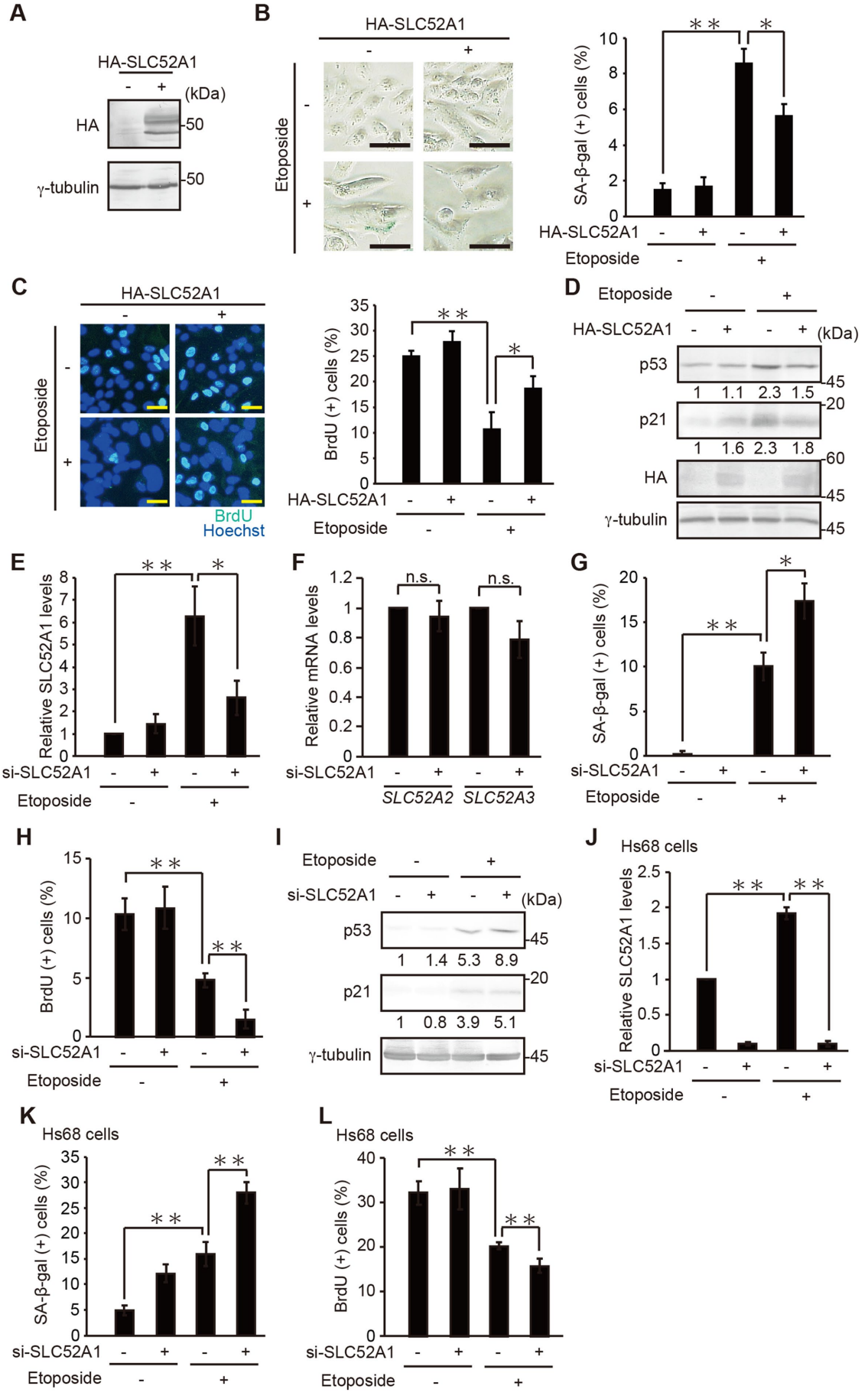
A
HA-SLC52A1
- +
(kDa)
HA
50
γ-tubulin
50
B
HA-SLC52A1
- +
Etoposide
- +
SA-β-gal (+) cells (%)
HA-SLC52A1
Etoposide
C
HA-SLC52A1
Etoposide
BrdU
Hoechst
BrdU (+) cells (%)
D
Etoposide
HA-SLC52A1
(kDa)
p53
45
1 1.1 2.3 1.5
p21
20
1 1.6 2.3 1.8
HA
60
45
γ-tubulin
45
E
Relative SLC52A1 levels
si-SLC52A1
Etoposide
F
Relative mRNA levels
n.s.
n.s.
si-SLC52A1
SLC52A2
SLC52A3
G
SA-β-gal (+) cells (%)
si-SLC52A1
Etoposide
H
BrdU (+) cells (%)
si-SLC52A1
Etoposide
I
Etoposide
si-SLC52A1
(kDa)
p53
45
1 1.4 5.3 8.9
p21
20
1 0.8 3.9 5.1
γ-tubulin
45
J
Hs68 cells
Relative SLC52A1 levels
si-SLC52A1
Etoposide
K
Hs68 cells
SA-β-gal (+) cells (%)
si-SLC52A1
Etoposide
L
Hs68 cells
BrdU (+) cells (%)
si-SLC52A1
Etoposide

inactivation of cyclin-dependent kinases (el-Deiry *et al.*, 1993; Romanov *et al.*, 2012), and proline dehydrogenase promotes senescence by enhancement of reactive oxygen species–mediated DNA damage (Nagano *et al.*, 2017). On the contrary, however, it remains unclear whether gene(s) that have antisenescence functions are also up-regulated by p53. In the case of p53-mediated apoptosis, the activated p53 up-regulates not only proapoptotic genes but also antiapoptotic genes, such as *EGFR*, *MDM2*, and *14-3-3δ*, which functions as a fail-safe mechanism against aberrant activation of the apoptotic machinery (Jänicke *et al.*, 2008). Recently, we have identified *SLC52A1* to be up-regulated by senescence-inducing stimuli in a p53-dependent manner and preliminarily observed that overexpression of SLC52A1 decreased some senescence markers (Nagano *et al.*, 2016). However, the precise mechanism by which SLC52A1 inhibits senescence is still unknown.

RESULTS AND DISCUSSION

SLC52A1 contributes to suppress DNA damage–induced senescence in tumor and normal cells

To examine the role of SLC52A1 in cellular senescence, we introduced an expression vector carrying *SLC52A1* into U2OS cells, a human osteosarcoma cell line, and the extent of senescence was evaluated by well-known senescence markers, SA-β-gal staining (Dimri *et al.*, 1995) and the BrdU proliferation assay (Figure 1, A–C). As previously reported (Nagano *et al.*, 2016), a sublethal dose (2 μM) of etoposide, a DNA damaging anticancer drug, effectively induced senescence in U2OS cells, as determined by the activation of SA-β-gal and the loss of proliferative capacity (Figure 1, B and C). Furthermore, overexpression of SLC52A1 impaired the etoposide-induced activation of SA-β-gal and partially reversed the loss of proliferative capacity. Moreover, etoposide-induced up-regulation of p53 and p21, widely observed in senescent cells, was impaired by SLC52A1 overexpression, although a slight increase in p21 was induced independently of p53 in SLC52A1-overexpressing cells (Figure 1D). These results raise the possibility that SLC52A1 is involved in the suppression of DNA damage–induced senescence.

To explore this possibility, we next tested the effect of *SLC52A1* knockdown on senescence. U2OS cells were transfected with a pool of four different *SLC52A1* small interfering RNAs (siRNAs), and the efficacy of *SLC52A1* knockdown was confirmed by quantitative PCR (qPCR) because we could not reproducibly detect the SLC52A1 protein by immunoblot analysis, possibly due to its low expression level under steady state conditions (Figure 1E). The *SLC52A1* expression level was up-regulated upon senescence as reported previously (Nagano *et al.*, 2016), which was effectively abolished by siRNA (Figure 1E). *SLC52A1* depletion did not affect the expression of the other SLC52A family genes (*SLC52A2* and *SLC52A3*) (Figure 1F). More importantly, knockdown of *SLC52A1* promoted the etoposide-induced activation of SA-β-gal and the loss of proliferative capability, while *SLC52A1* knockdown alone had no significant effect (Figure 1, G and H). The etoposide-induced increase in p53 and p21 was also enhanced by *SLC52A1* knockdown (Figure 1I). Furthermore, to evaluate the generality of the findings, we included normal human fibroblast Hs68 cells in the analyses. As is the case in U2OS cells, the *SLC52A1* expression was up-regulated by the treatment with a sublethal dose of etoposide (0.5 μM) in Hs68 cells, which was abrogated by siRNA against *SLC52A1* (Figure 1J). In addition, the SA-β-gal activation and loss of proliferative capacity were effectively induced by etoposide, and *SLC52A1* depletion promoted these senescence biomarkers (Figure 1, K and L). These results suggest that SLC52A1 contributes to suppress DNA damage–induced senescence in both tumor and normal cells.

Senescence suppression by SLC52A1 is mediated by riboflavin incorporation

Because SLC52A1 acts as a transporter of riboflavin (Yonezawa and Inui, 2013), we investigated whether supplementation of riboflavin to culture medium inhibits the senescence markers. The extent of etoposide-induced SA-β-gal activation in U2OS cells cultured in conventional DMEM (containing 1 μM riboflavin) was compared with that in cells cultured in DMEM supplemented with 25–100 μM riboflavin (Figure 2A). As a result, riboflavin supplementation effectively decreased the levels of SA-β-gal activity, which was most prominent when supplemented with 50 μM (Figure 2A). Furthermore, the etoposide-induced up-regulation of p53 and p21 was impaired by the supplementation with riboflavin (Figure 2B). The riboflavin supplementation also effectively suppressed the etoposide-induced SA-β-gal activation and loss of proliferative capacity in normal Hs68 cells (Figure 2, C and D). Moreover, to examine the riboflavin effect on replicative senescence, Hs68 cells with different passage numbers (passages 37, 42, and 47–48 as representatives of early, middle, and late passage cells, respectively) were treated with riboflavin (Figure 2, E and F). Riboflavin impaired the SA-β-gal activation and the loss of proliferative capacity in the middle passage, while no effect was observed in the late passage (Figure 2, E and F). These results raise the possibility that an increase in riboflavin uptake has an antisenescence effect at a relatively early stage. Whereas SLC52A1 overexpression in combination with the riboflavin supplementation did not show any additive effect on the senescence markers (Figure 2, G and H), lumiflavin, a riboflavin analogue that inhibits the riboflavin transport activity (Yonezawa *et al.*, 2008), markedly reversed the effect of SLC52A1 overexpression on senescence markers in a dose-dependent manner (Figure 2, I and J). Collectively, these results suggest that the effect of SLC52A1 on senescence suppression is mediated by riboflavin transport activity.

FIGURE 1: SLC52A1 contributes to suppress DNA damage–induced senescence in tumor and normal cells. (A) U2OS cells transfected with pcDNA3-HA-SLC52A1 were subjected to immunoblot analysis. (B, C) SLC52A1-overexpressing U2OS cells treated with 2 μM etoposide for 7 d were subjected to SA-β-gal (B) and BrdU (C) assays. Representative microscopic images (B and C, left panels) and the percentage of SA-β-gal–positive cells (B, right panel) and BrdU-positive cells (C, right panel) are shown. Bars, 50 μm. (D) SLC52A1-overexpressing U2OS cells treated with 2 μM etoposide for 5 d were subjected to immunoblot analysis. The protein levels relative to the γ-tubulin level were quantified using NIH ImageJ software. (E–H) U2OS cells transfected with siRNA for *SLC52A1* and treated with 2 μM etoposide for 7 d were subjected to qPCR (E, F), SA-β-gal (G), and BrdU (H) assays. (F) Gene expressions of *SLC52A2* and *SLC52A3* in *SLC52A1*-depleted cells treated with etoposide were examined by qPCR. (I) *SLC52A1*-depleted U2OS cells treated with 2 μM etoposide for 5 d were subjected to immunoblot analysis. (J–L) Hs68 cells transfected with siRNA for *SLC52A1* and treated with 0.5 μM etoposide for 7 d were subjected to qPCR (J), SA-β-gal (K), and BrdU (L) assays. Data are mean ± SD ($n = 3$ independent cultures). Statistical significance is shown using Student's *t* test analysis; $^{*}P < 0.05$; $^{**}P < 0.01$.

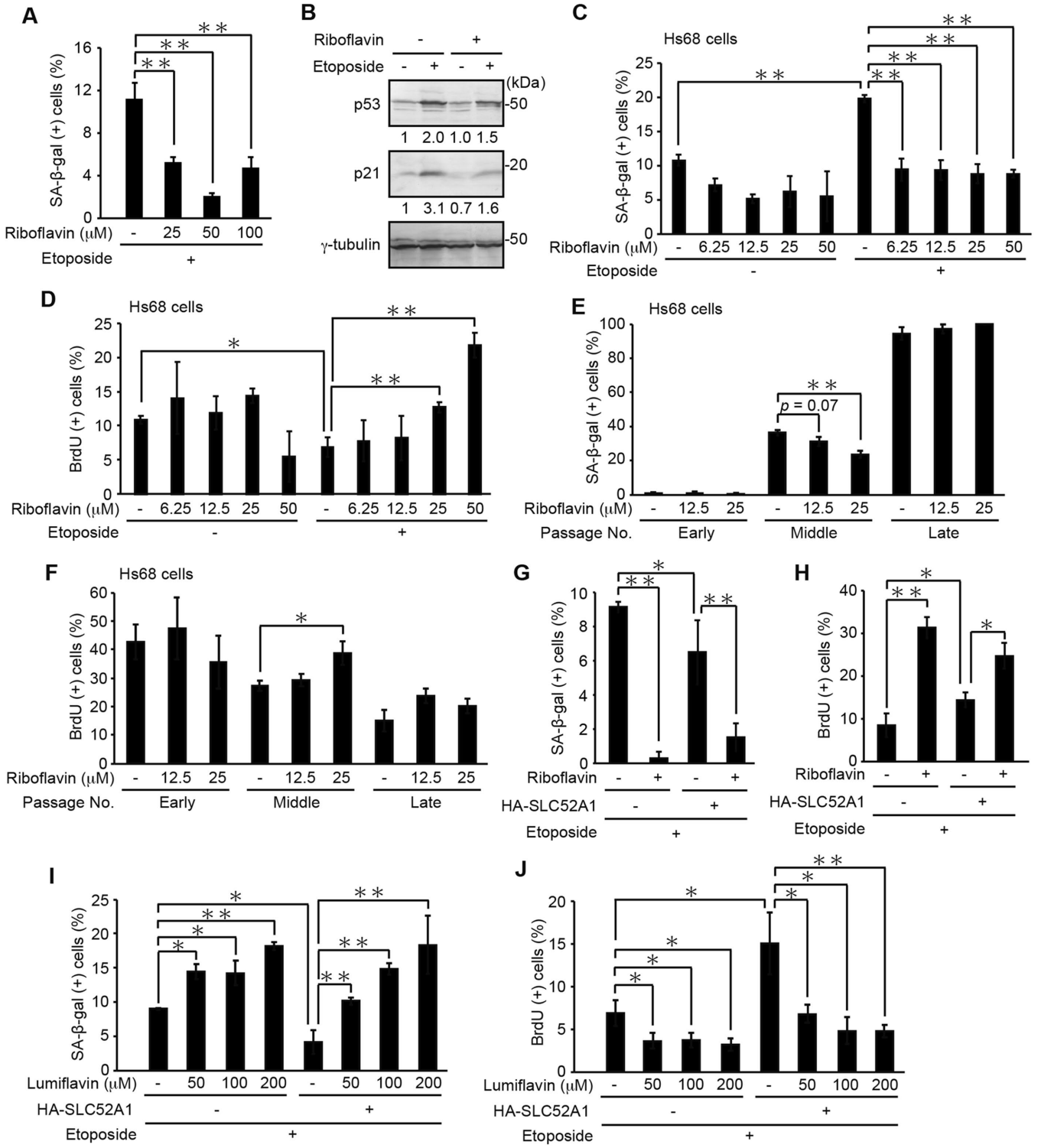

FIGURE 2: Senescence suppression by SLC52A1 is mediated by riboflavin incorporation. (A) U2OS cells treated with 2 μM etoposide and the indicated concentrations of riboflavin for 7 d were subjected to SA-β-gal staining. The percentages of SA-β-gal–positive cells are shown. (B) U2OS cells treated with 50 μM riboflavin and 2 μM etoposide for 5 d were subjected to immunoblot analysis. The protein levels relative to the γ-tubulin level were quantified using NIH ImageJ software. (C, D) Hs68 cells treated with 0.5 μM etoposide and riboflavin for 7 d were subjected to SA-β-gal (C) and BrdU (D) assays. The percentages of SA-β-gal–positive cells (C) and BrdU-positive cells (D) are shown. (E, F) Hs68 cells at early (P37), middle (P42), and late (P47–48) passage numbers treated with riboflavin for 7 d were subjected to SA-β-gal (E) and BrdU (F) assays. (G, H) U2OS cells transfected with pcDNA3-HA-SLC52A1 and treated with 2 μM etoposide and 50 μM riboflavin for 7 d were subjected to SA-β-gal (G) and BrdU (H) assays. (I, J) U2OS cells treated with 2 μM etoposide and the indicated concentrations of lumiflavin for 7 d were subjected to SA-β-gal (I) and BrdU (J) assays. Data are mean ± SD ($n = 3$ independent cultures). Statistical significance is shown using Student's t test analysis; *$P < 0.05$; **$P < 0.01$.

Riboflavin suppresses senescence through the activation of mitochondrial ETC complex II

In cells, riboflavin is metabolically converted to FAD, which catalyzes a lot of redox reactions. Given the up-regulation of *SLC52A1* in response to etoposide (Figure 1, E and J), it is possible that intracellular FAD concentrations are elevated during DNA damage–induced senescence, thereby leading to changes in the activity of FAD-dependent redox enzymes. In fact, FAD levels were observed to increase in both U2OS and normal Hs68 cells upon senescence, which was abrogated by knockdown of *SLC52A1* (Figure 3, A and B). Because FAD is required for several key biological processes in mitochondria, such as oxidative phosphorylation via the ETC (Udhayabanu *et al.*, 2017), we assessed mitochondrial activity in the cells treated with etoposide. To this end, mitochondrial membrane potential (MMP) was monitored by using an MMP-dependent fluorescent dye, MitoTracker CMXRos (Pendergrass *et al.*, 2004). We observed that MMP was increased in response to etoposide with a peak at 5 d in U2OS cells (Figure 3C). Furthermore, the etoposide-induced MMP activation was abrogated by knockdown of *SLC52A1* (Figure 3D), which was also observed in normal Hs68 cells (Figure 3E). Given that inactivation of mitochondria leads to senescence (Campisi 2013; Salama *et al.*, 2014; Wiley *et al.*, 2016; Abate *et al.*, 2020), the increase in MMP upon the etoposide treatment is possibly responsible for the riboflavin-mediated senescence suppression. To test this possibility, we investigated the effects of riboflavin supplementation on MMP. MMP was remarkably enhanced by the riboflavin supplementation (Figure 3F). Conversely, the etoposide-induced MMP elevation was completely abolished by lumiflavin (Figure 3G), suggesting that the increase in riboflavin uptake upon senescence leads to the MMP activation. MMP is predominantly produced by the electron flow through ETC complexes I–IV (Bagkos *et al.*, 2014), and among the ETC complexes, complex II contains FAD-dependent succinate dehydrogenase (Cecchini, 2003), raising the possibility that the senescence-associated increase in FAD level activates complex II. Therefore, we investigated whether complex II mediates the senescence-associated MMP activation. Thenoyltrifluoroacetone (TTFA), a conventional complex II inhibitor, effectively inhibited the etoposide-induced MMP activation in U2OS and Hs68 cells (Figure 3, H and I). In addition, the inhibitory effect of TTFA on MMP was also confirmed when MMP was activated by the riboflavin supplementation (Figure 3J). These results indicate that the MMP elevation upon etoposide treatment is dependent on complex II activity. Furthermore, the TTFA treatment alone modestly induced the SA-β-gal activity and loss of proliferative capacity, and when combined with etoposide, it enhanced these senescence markers (Figure 3, K and L). Additionally, and most importantly, suppression of these senescence markers by SLC52A1 overexpression was significantly impaired by TTFA, although the effect on SA-β-gal was only modest (Figure 3, K and L). TTFA also enhanced the etoposide-induced increase in p21 (Figure 3M). Moreover, a simultaneous analysis of SA-β-gal and MMP in the same cell revealed that MMP was significantly higher in the SA-β-gal–negative cells than in the SA-β-gal–positive cells in the presence and absence of TTFA (Figure 3N). These results suggest that senescence suppression by SLC52A1 is mediated, at least in part, through the activation of mitochondria ETC complex II.

Complex II–mediated mitochondrial activation attenuates the AMPK-p53 pathway

Because mitochondrial dysfunction has been shown to activate AMPK through elevation of the intracellular AMP/ATP ratio, which phosphorylates and activates p53 and consequently induces senescence (Wiley *et al.*, 2016; Abate *et al.*, 2020), we examined the AMPK activity in etoposide-treated cells (Figure 4A). Although AMPK activity itself was largely unchanged during senescence, it was slightly decreased by overexpression of SLC52A1, as determined by the phosphorylation level of AMPK at Thr172 (Figure 4A). In response to DNA damage, p53 is phosphorylated at N-terminal serines by several kinases. For example, AMPK phosphorylates p53 at Ser15, leading to p53 stabilization and activation (Vousden and Prives, 2009; Rufini *et al.*, 2013). In line with this, the phosphorylation level of p53 relative to its total protein level was increased by etoposide, which was impaired by SLC52A1 overexpression (Figure 4A), suggesting that phosphorylation of AMPK and p53 was inhibited by SLC52A1 overexpression. To evaluate whether this inhibitory effect on AMPK-p53 pathway is mediated by the ETC complex II activity, we tested the effects of TTFA on the AMPK-p53 activity in U2OS and Hs68 cells (Figure 4, B and C). Although the phosphorylation levels of AMPK were increased by TTFA regardless of the presence of etoposide, the p53 phosphorylation levels were more potently increased by the combined treatment with etoposide and TTFA than with etoposide alone in both cell lines (Figure 4, B and C). These results suggest that phosphorylation of AMPK and p53 is impaired by complex II–dependent mitochondrial activation, which can serve as a negative feedback mechanism that limits excessive p53 activation following DNA damage (Figure 4D).

It is increasingly clear that mitochondrial dysfunctions promote senescence, and senescent cells show significant alterations in energy metabolism (Wiley *et al.*, 2016; Abate *et al.*, 2020). MMP is known to be decreased as a consequence of the establishment of senescence (Passos *et al.*, 2010). However, the detailed changes in mitochondrial activity upon senescence induction are still ambiguous. Wang *et al.* (2016) have shown that mitochondrial activity (i.e., MMP, ATP production, and respiratory rate) is transiently increased by senescence-inducing stimuli, but it is unclear whether this mitochondrial activation contributes to suppress senescence or not. Our results showed that inhibition of MMP activation impaired the antisenescence effect of SLC52A1, suggesting that SLC52A1 suppresses senescence at least partially mediated by MMP elevation.

How does the MMP increase contribute to senescence suppression? Mitochondrial uncouplers (FCCP, niclosamide, etc.) that dissipate MMP by promoting proton leak across the mitochondrial inner membrane have been reported to activate AMPK through the decrease in intracellular ATP levels (Tao *et al.*, 2014). AMPK is a cellular energy sensor whose activity is directly linked to the energy state of the cell and plays a critical role in cell proliferation through the regulation of downstream transcription factors, including p53 (Jones *et al.*, 2005). Cells show high energy demand to increase the cell size and produce senescence-associated secretory proteins during the transition from proliferation to senescence (Wang *et al.*, 2003; Salama *et al.*, 2014). Because mitochondria play a key role in matching energy supply with the high energy demand in these responses (Kim *et al.*, 2018), the SLC52A1-dependent MMP increase possibly contributes to prevent AMPK activation by supporting the increased energy demands following the exposure to senescence-inducing stimuli. We observed that AMPK was activated by complex II inhibition by TTFA, and etoposide-induced activation of p53 was potentiated by TTFA, suggesting that complex II–mediated mitochondrial activation limits further activation of p53 presumably by keeping AMPK inactive. However, this mechanism does not fully explain the antisenescence function of SLC52A1 because senescence was still suppressed by SLC52A1 overexpression even in the presence of TTFA (Figure 3, K and L). Other FAD-dependent enzyme(s) can also contribute to the regulation of senescence because the human

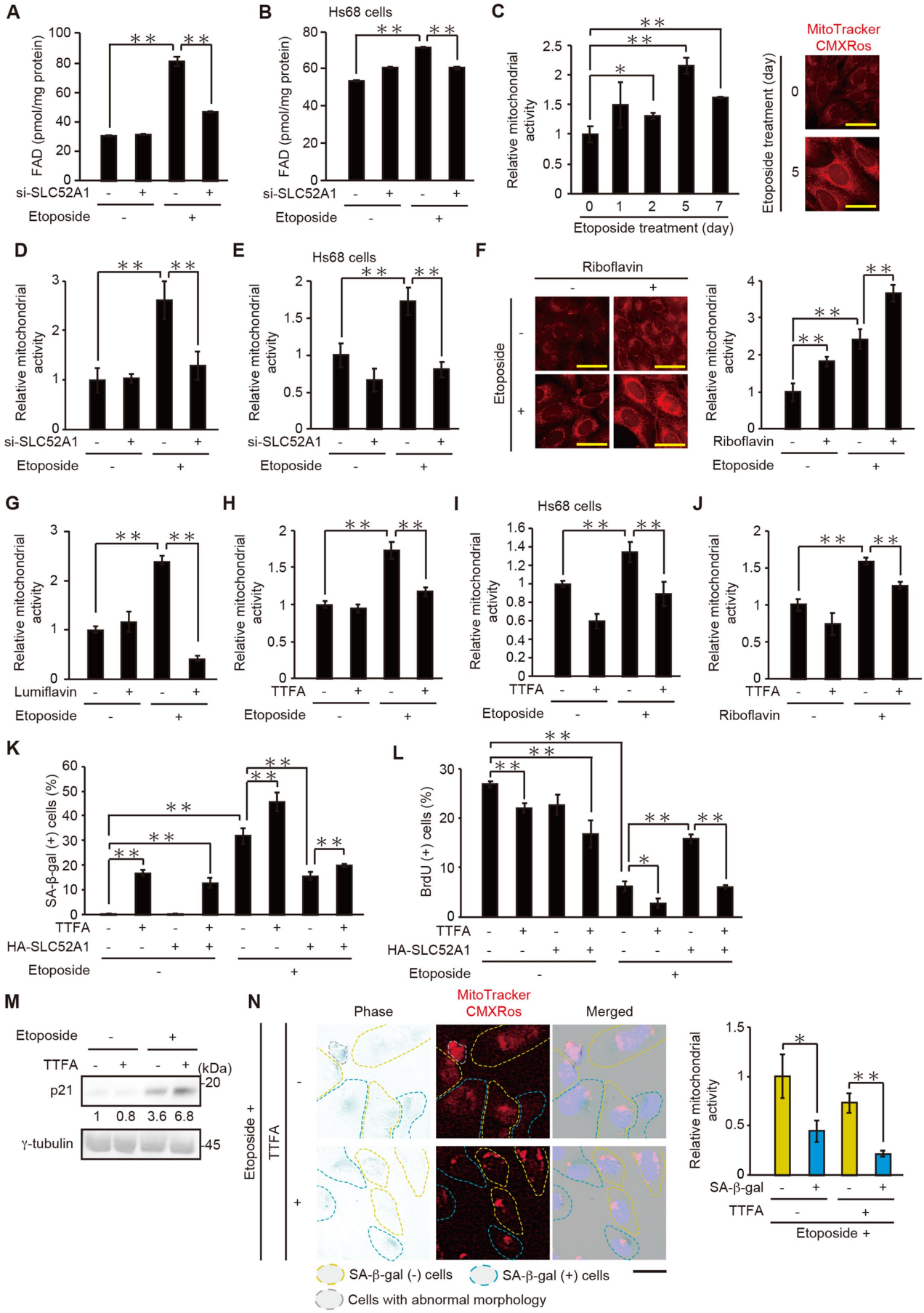
A
FAD (pmol/mg protein)
si-SLC52A1
Etoposide
B
Hs68 cells
C
Relative mitochondrial activity
Etoposide treatment (day)
MitoTracker CMXRos
D
E
F
Riboflavin
G
Lumiflavin
H
I
J
K
SA-β-gal (+) cells (%)
TTFA
HA-SLC52A1
L
BrdU (+) cells (%)
M
p21
γ-tubulin
(kDa)
1 0.8 3.6 6.8
N
Phase
Merged
SA-β-gal (-) cells
SA-β-gal (+) cells
Cells with abnormal morphology

genome contains 64 genes encoding FAD-dependent enzymes (Lienhart *et al.*, 2013). Nevertheless, our results clearly show a novel function of SLC52A1 as a negative feedback mechanism for the induction of p53-dependent senescence, which may shed new light on the riboflavin roles in the regulation of senescence.

MATERIALS AND METHODS

Request a protocol through *Bio-protocol*.

Cell culture, treatment, and transfection

U2OS (a human osteosarcoma line; American Type Culture Collection, Rockville, MD) and Hs68 (normal human diploid fibroblasts; IFO50350; JCRB Cell Bank, Osaka, Japan) cells were cultured in DMEM (Wako, Osaka, Japan) supplemented with 10% fetal bovine serum. The cells were treated with etoposide (Sigma Aldrich, St. Louis, MO) to induce DNA double-strand breaks. For senescence induction, U2OS and Hs68 cells were treated with 2 and 0.5 μM etoposide (Sigma Aldrich), respectively, for 48 h and further cultured in DMEM without etoposide for an additional 5 d to develop senescence phenotypes (Nakano *et al.*, 2013; Nagano *et al.*, 2016, 2019). Transfection with expression vectors was carried out by using Effectene Transfection Reagent (Qiagen, Venlo, the Netherlands) according to the manufacturer's instructions. The transfected cells were selected by 800 μg/ml of the neomycin analogue G418 (Wako) for 5 d. Riboflavin (Nacalai Tesque, Kyoto, Japan) was added at the indicated concentrations. To inhibit riboflavin uptake, cells were incubated with 50–200 μM lumiflavin (Sigma Aldrich). When TTFA (Focus Biomolecules, Plymouth Meeting, PA) was used, the reagent was added at 400 μM. Stock solutions of etoposide and TTFA were prepared in dimethyl sulfoxide, whereas riboflavin and lumiflavin were dissolved in 100 mM NaOH.

Plasmid constructions

For the construction of pcDNA3-HA-SLC52A1, an expression vector for N-terminal HA-tagged human full-length SLC52A1 (NCBI Reference Sequence: NM_001104577.2), the cDNA fragment of *SLC52A1* was amplified with a pair of primers (a forward primer: 5′-CGTGCTCGGAATTCATGGCAGCACCCACGCT-3′ and a reverse primer: 5′-CGTGATAGGCGGCCGCTCAGGGGCCACAGGGGT-3′) using a plasmid containing PAR2 (SLC52A1) cDNA (kindly provided by Y. Takeuchi, University College London, UK) as a template. The resulting PCR fragment was digested with *Eco*RI and *Not*I and cloned into the pcDNA3 vector (Invitrogen, Carlsbad, CA).

Immunoblot analysis

The cells were lysed in lysis buffer (1% Triton X-100, 20 mM Tris-HCl [pH 7.5], 1 mM EDTA, 150 mM NaCl, 20 mM NaF, 10 μg/ml leupeptin, 10 μg/ml aprotinin, 1 mM *p*-amidinophenylmethanesulfonyl fluoride-HCl, 1 mM Na_3VO_4), and the lysates were separated by SDS–PAGE and blotted onto Immobilon polyvinylidene difluoride membrane (Merck Millipore, Darmstadt, Germany). Each protein was detected using primary antibodies as indicated, alkaline phosphatase (AP)-conjugated secondary antibodies, and the chromogenic NBT/BCIP (Nacalai Tesque) substrates.

Antibodies

Anti-p53 antibody (sc-126; 1:1000) and AP-conjugated anti-rat antibody (sc-2021; 1:2500) were obtained from Santa Cruz Biotechnology (Santa Cruz, CA); anti–phospho-AMPK (The172) antibody (#2535; 1:1000) and anti–phospho-p53 (Ser15) antibody (#9284; 1:1000) were from Cell Signaling Technology (Beverly, MA); AP-conjugated anti-mouse antibody (S372B; 1:2500) and AP-conjugated anti-rabbit antibody (S373B; 1:2500) were from Promega (Madison, WI); anti-HA 3F10 monoclonal antibody (1867423; 1:1000) was from Roche (Basel, Switzerland); anti–γ-tubulin antibody (T6557; 1:2000) was from Sigma Aldrich; anti-p21 antibody (K0081-3; 1:500) was from Medical and Biological Laboratories Co., Ltd. (Nagoya, Japan); anti-AMPK α1 antibody (07-350; 1:1000) was from Merck Millipore

Senescence assay

To measure SA-β-gal activity, the Senescence β-Galactosidase staining kit (Cell Signaling Technology) was used according to the manufacturer's instructions. Briefly, the cells were fixed with 2% formaldehyde/0.2% glutaraldehyde for 15 min and then stained with SA-β-Gal staining solution (1 mg/ml 5- bromo-4-chloro-3-indolyl-β-D-galactoside, 40 mM citric acid/sodium phosphate [pH 6.0], 5 mM potassium ferrocyanide, 5 mM potassium ferricyanide, 150 mM NaCl, 2 mM $MgCl_2$) for 24 h at 37°C. The stained cells were examined under a fluorescence microscope (model BZ-8000; Keyence, Osaka, Japan), and blue-stained cells were identified as senescent. For the BrdU incorporation proliferation assay, the cells were labeled with 10 μM BrdU (Sigma Aldrich) for 3 h (U2OS cells) or 24 h (Hs68 cells), fixed with 3.7% formaldehyde, and permeabilized with 0.5% Triton X-100. DNA was hydrolyzed by exposing cells to 2 M HCl for 10 min, and the cells were incubated with anti-BrdU antibody (BD Pharmingen; 555627; 1:400) overnight at 4°C followed by incubation with Alexa Fluor 488–conjugated secondary antibodies

FIGURE 3: Riboflavin suppresses senescence through the activation of mitochondrial ETC complex II. (A, B) U2OS (A) and Hs68 (B) cells transfected with siRNA for *SLC52A1* and treated with 2 and 0.5 μM etoposide, respectively, for 5 d were subjected to measurement of intracellular FAD levels. (C) U2OS cells treated with 2 μM etoposide for the indicated periods were stained with 250 nM MitoTracker and observed under a fluorescence microscope. Relative mitochondrial activity determined by fluorescence intensity of MitoTracker (left) and representative microscopic images (right) are shown. Bars, 50 μm. (D, E) U2OS (D) and Hs68 (E) cells treated with 2 and 0.5 μM etoposide, respectively, for 5 d were subjected to measurement of mitochondrial activity. (F–H) U2OS cells treated with 2 μM etoposide alone or in combination with 50 μM riboflavin (F), 200 μM lumiflavin (G), and 400 μM TTFA (H) for 5 d were subjected to measurement of mitochondrial activity. (F) Representative microscopic images (left) and relative mitochondrial activity (right) are shown. Bars, 50 μm. (I) Hs68 cells treated as in H were subjected to measurement of mitochondrial activity. (J) U2OS cells treated with 400 μM TTFA and 50 μM riboflavin for 5 d were subjected to measurement of mitochondrial activity. (K, L) U2OS cells transfected with pcDNA3-HA-SLC52A1 and treated with 2 μM etoposide and 400 μM TTFA for 7 d were subjected to SA-β-gal (K) and BrdU (L) assays. (M, N) U2OS cells treated with 2 μM etoposide and 400 μM TTFA for 5 d were subjected to immunoblot analysis (M) and simultaneous analysis of SA-β-gal and mitochondrial activity (N). (M) The protein levels relative to the γ-tubulin level were quantified using NIH ImageJ software. (N) Representative microscopic images (left) and comparison of mitochondrial activity between SA-β-gal–negative (–) and –positive (+) cells (right) are shown. Bar, 50 μm. Data are mean ± SD ($n = 3$ independent cultures). Statistical significance is shown using Student's *t* test analysis; $^*P < 0.05$; $^{**}P < 0.01$.

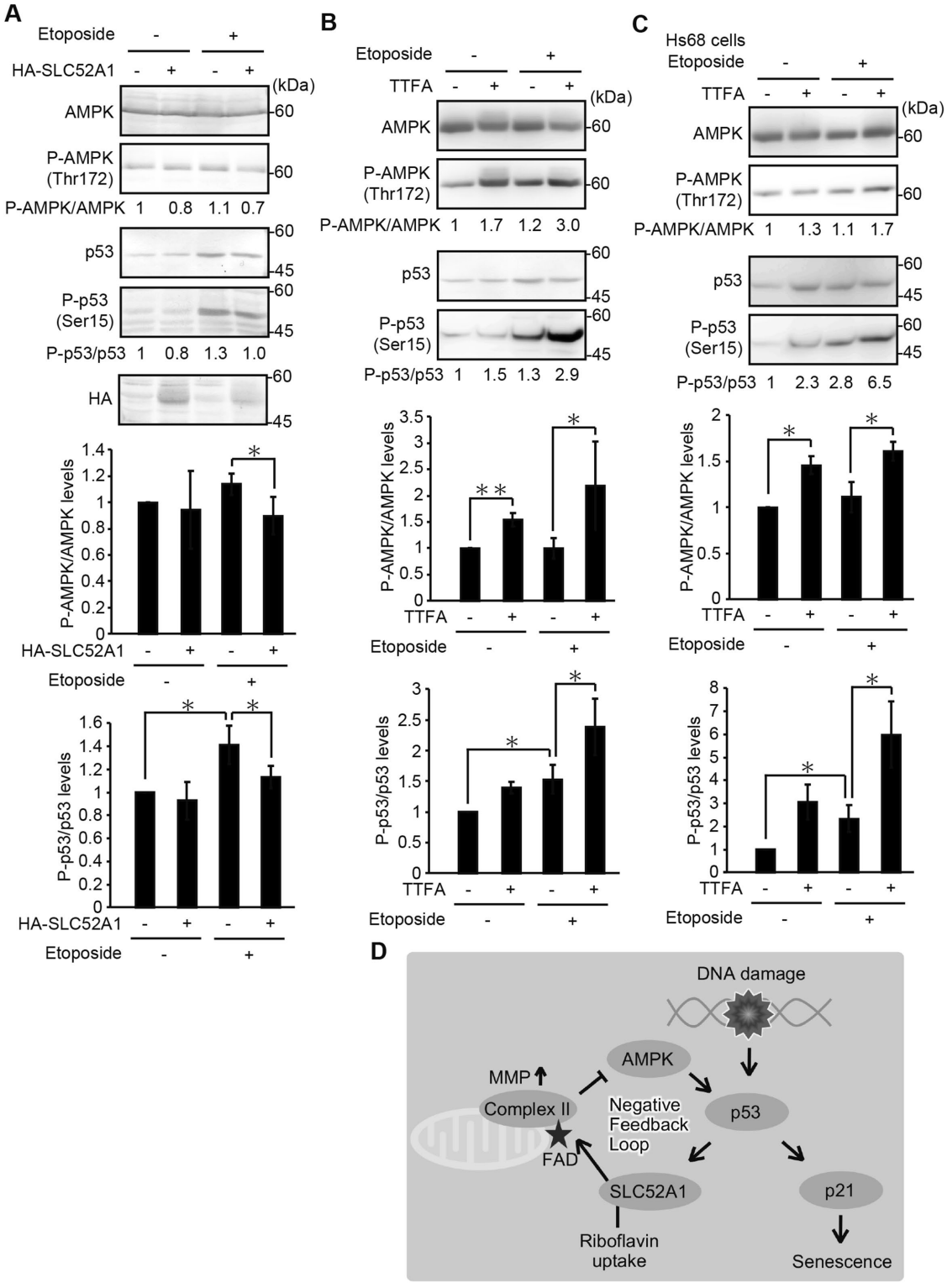

FIGURE 4: Complex II–mediated mitochondrial activation attenuates the AMPK-p53 pathway. (A) U2OS cells transfected with pcDNA3-HA-SLC52A1 and treated with 2 μM etoposide for 5 d were subjected to immunoblot analysis. The phosphorylation levels of AMPK and p53 relative to their total protein levels were quantified using NIH ImageJ software. Representative immunoblot images from replicate experiments ($n = 3$, top panels) and the results of their statistical analysis (bottom panels) are shown. (B, C) U2OS (B) and Hs68 (C) cells treated with 400 μM TTFA and etoposide at 2 and 0.5 μM, respectively, for 5 d were subjected to immunoblot analysis as in A. (D) Schematic model of SLC52A1-mediated negative feedback regulation of p53. SLC52A1 contributes to increase riboflavin uptake upon DNA damage, which leads to MMP activation and consequently suppresses the AMPK-p53 pathway to prevent p53-dependent senescence. Data are mean ± SD ($n = 3$ independent cultures). Statistical significance is shown using Student's *t* test analysis; $^{*}P < 0.05$; $^{**}P < 0.01$.

(ThermoFisher Scientific, Waltham, MA; A-11029) for 1 h at room temperature. After the nuclei were stained with 10 μM Hoechst 33342, the cells were observed under a fluorescence microscope (model BZ-9000; Keyence). At least 100 cells in randomly selected microscopic fields were counted to determine the percentage of SA-β-gal–positive cells and BrdU-positive cells.

RNA interference

ON-TARGETplus Smart Pool siRNA for *SLC52A1* (L-010712-00) and its control siRNA (D-001810-10) were from Dharmacon Horizon Discovery (Lafayette, CO). U2OS and Hs68 cells were seeded and transfected with 30 nM siRNA using Lipofectamin RNAiMAX Transfection Reagent (ThermoFisher Scientific) according to the manufacturer's instructions.

RNA isolation and qPCR

Total RNA was isolated from siRNA-transfected U2OS and Hs68 cells using the RNeasy Mini Kit (Qiagen) according to the manufacturer's instructions. cDNA was synthesized using the ReverTra Ace qPCR RT Master Mix with gDNA Remover (TOYOBO, Osaka, Japan) and subjected to qPCR (LightCycler480 Real-Time PCR System; Roche Life Science, Penzberg, Germany) using specific primers for *GAPDH* (a forward primer: 5′-CAATGACCCCTTCATTGACCT-3′ and a reverse primer: 5′-ATGACAAGCTTCCCGTTCTC-3′), *SLC52A1* (a forward primer: 5′-TTGCTGTTGCCATCACTACC-3′ and a reverse primer: 5′-CAAAGCCTCTTCTTCCTCCTTC-3′), *SLC52A2* (a forward primer: 5′-CCACCTGACGCTAGAAGAAGT-3′ and a reverse primer: 5′-TTGGCTCTCCTGGGAAGTGA-3′), and *SLC52A3* (a forward primer: 5′-CGGACCTCGTCTCCCATCTA-3′ and a reverse primer: 5′-ACGCTAACTGGGCCAATCTT-3′). Relative expression levels were calculated by the 2^(ΔΔCt) method (ΔCt sample – ΔCt calibrator).

FAD measurement

FAD measurement was performed using the FAD Assay Kit (ab204710; Abcam, Cambridge, UK) according to the manufacturer's instructions. Briefly, the cells were lysed and deproteinized with $HClO_4$, and the resulting samples were mixed with the reaction mixture. The concentration of FAD was measured by a colorimetric assay at 570 nm based on the FAD-dependent reaction of an OxiRed probe using a spectrophotometer (iMark microplate reader; Bio-Rad, Hercules, CA).

Assessment of MMP

To assess MMP, the cells were incubated with 250 nM MitoTracker Red CMXRos (ThermoFisher Scientific) for 30 min and observed under a fluorescence microscope (model BZ-9000; Keyence). The mean MitoTracker fluorescence intensity was quantified by ImageJ (National Institutes of Health [NIH]) software. When both MMP and SA-β-gal were simultaneously analyzed, the cells were treated with MitoTracker followed by staining of SA-β-gal using the Senescence β-Galactosidase staining kit as described above, and at least 10 cells in randomly selected microscopic fields were counted to determine the relative mitochondrial activity.

Statistical analysis

The two-tailed Student's *t* test was used to calculate *P* values for all data sets.

ACKNOWLEDGMENTS

We thank Y. Takeuchi for providing the PAR2 (SLC52A1) plasmid. This work was supported by Japan Society for the Promotion of Science (JSPS) KAKENHI Grant Numbers 25640063, 17K15595, 20K07591, and 20K15791, The Uehara Memorial Foundation, Japan, and a Leave a Nest Grant from Leave a Nest Co., Ltd., Japan.

REFERENCES

Abate M, Festa A, Falco M, Lombardi A, Luce A, Grimaldi A, Zappavigna S, Sperlongano P, Irace C, Caraglia M, Misso G (2020). Mitochondria as playmakers of apoptosis, autophagy and senescence. Semin Cell Dev Biol 98, 139–153.

Bagkos G, Koufopoulos K, Piperi C (2014). A new model for mitochondrial membrane potential production and storage. Med Hypotheses 83, 175–181.

Campisi J (2013). Aging, cellular senescence, and cancer. Annu Rev Physiol 75, 685–705.

Cecchini G (2003). Function and structure of complex II of the respiratory chain. Annu Rev Biochem 72, 77–109.

Dimri GP, Lee X, Basile G, Acosta M, Scott G, Roskelley C, Medrano EE, Linskens M, Rubelj I, Pereira-Smith O, *et al.* (1995). A biomarker that identifies senescent human cells in culture and in aging skin in vivo. Proc Natl Acad Sci USA 92, 9363–9367.

el-Deiry WS, Tokino T, Velculescu VE, Levy DB, Parsons R, Trent JM, Lin D, Mercer WE, Kinzler KW, Vogelstein B (1993). WAF1, a potential mediator of p53 tumor suppression. Cell 75, 817–825.

Fagerberg L, Hallström BM, Oksvold P, Kampf C, Djureinovic D, Odeberg J, Habuka M, Tahmasebpoor S, Danielsson A, Edlund K, *et al.* (2014). Analysis of the human tissue-specific expression by genome-wide integration of transcriptomics and antibody-based proteomics. Mol Cell Proteomics 13, 397–406.

Ho G, Yonezawa A, Masuda S, Inui K, Sim KG, Carpenter K, Olsen RK, Mitchell JJ, Rhead WJ, Peters G, *et al.* (2011). Maternal riboflavin deficiency, resulting in transient neonatal-onset glutaric aciduria Type 2, is caused by a microdeletion in the riboflavin transporter gene GPR172B. Hum Mutat 32, E1976–E1984.

Jänicke RU, Sohn D, Schulze-Osthoff K (2008). The dark side of a tumor suppressor: anti-apoptotic p53. Cell Death Differ 15, 959–976.

Jones RG, Plas DR, Kubek S, Buzzai M, Mu J, Xu Y, Birnbaum MJ, Thompson CB (2005). AMP-activated protein kinase induces a p53-dependent metabolic checkpoint. Mol Cell 18, 283–293.

Kim SJ, Mehta HH, Wan J, Kuehnemann C, Chen J, Hu JF, Hoffman AR, Cohen P (2018). Mitochondrial peptides modulate mitochondrial function during cellular senescence. Aging (Albany NY) 10, 1239–1256.

Lienhart WD, Gudipati V, Macheroux P (2013). The human flavoproteome. Arch Biochem Biophys 535, 150–162.

Nagano T, Nakano M, Nakashima A, Onishi K, Yamao S, Enari M, Kikkawa U, Kamada S (2016). Identification of cellular senescence-specific genes by comparative transcriptomics. Sci Rep 6, 31758.

Nagano T, Nakashima A, Onishi K, Kawai K, Awai Y, Kinugasa M, Iwasaki T, Kikkawa U, Kamada S (2017). Proline dehydrogenase promotes senescence through the generation of reactive oxygen species. J Cell Sci 130, 1413–1420.

Nagano T, Yamao S, Terachi A, Yarimizu H, Itoh H, Katasho R, Kawai K, Nakashima A, Iwasaki T, Kikkawa U, *et al.* (2019). D-amino acid oxidase promotes cellular senescence via the production of reactive oxygen species. Life Sci Alliance 2, e201800045.

Nakano M, Nakashima A, Nagano T, Ishikawa S, Kikkawa U, Kamada S (2013). Branched-chain amino acids enhance premature senescence through mammalian target of rapamycin complex I-mediated upregulation of p21 protein. PLoS One 8, e80411.

Passos JF, Nelson G, Wang C, Richter T, Simillion C, Proctor CJ, Miwa S, Olijslagers S, Hallinan J, Wipat A, *et al.* (2010). Feedback between p21 and reactive oxygen production is necessary for cell senescence. Mol Syst Biol 6, 347.

Pendergrass W, Wolf N, Poot M (2004). Efficacy of MitoTracker Green and CMXrosamine to measure changes in mitochondrial membrane potentials in living cells and tissues. Cytometry A 61, 162–169.

Powers HJ (2003). Riboflavin (vitamin B-2) and health. Am J Clin Nutr 77, 1352–1360.

Romanov VS, Pospelov VA, Pospelova TV (2012). Cyclin-dependent kinase inhibitor p21(Waf1): contemporary view on its role in senescence and oncogenesis. Biochemistry (Mosc) 77, 575–584.

Rufini A, Tucci P, Celardo I, Melino G (2013). Senescence and aging: the critical roles of p53. Oncogene 32, 5129–5143.

Salama R, Sadaie M, Hoare M, Narita M (2014). Cellular senescence and its effector programs. Genes Dev 28, 99–114.

Spaan AN, Ijlst L, van Roermund CW, Wijburg FA, Wanders RJ, Waterham HR (2005). Identification of the human mitochondrial FAD transporter

and its potential role in multiple acyl-CoA dehydrogenase deficiency. Mol Genet Metab 86, 441–447.
Tao H, Zhang Y, Zeng X, Shulman GI, Jin S (2014). Niclosamide ethanolamine-induced mild mitochondrial uncoupling improves diabetic symptoms in mice. Nat Med 20, 1263–1269.
Udhayabanu T, Manole A, Rajeshwari M, Varalakshmi P, Houlden H, Ashokkumar B (2017). Riboflavin responsive mitochondrial dysfunction in neurodegenerative diseases. J Clin Med 6, 52.
Vousden KH, Prives C (2009). Blinded by the light: the growing complexity of p53. Cell 137, 413–431.
Wang D, Liu Y, Zhang R, Zhang F, Sui W, Chen L, Zheng R, Chen X, Wen F, Ouyang HW, *et al*. (2016). Apoptotic transition of senescent cells accompanied with mitochondrial hyper-function. Oncotarget 7, 28286–28300.
Wang W, Yang X, López de Silanes I, Carling D, Gorospe M (2003). Increased AMP:ATP ratio and AMP-activated protein kinase activity during cellular senescence linked to reduced HuR function. J Biol Chem 278, 27016–27023.
Wiley CD, Velarde MC, Lecot P, Liu S, Sarnoski EA, Freund A, Shirakawa K, Lim HW, Davis SS, Ramanathan A, *et al*. (2016). Mitochondrial dysfunction induces senescence with a distinct secretory phenotype. Cell Metab 23, 303–314.
Yonezawa A, Masuda S, Katsura T, Inui K (2008). Identification and functional characterization of a novel human and rat riboflavin transporter, RFT1. Am J Physiol Cell Physiol 295, C632–C641.
Yonezawa A, Inui K (2013). Novel riboflavin transporter family RFVT/SLC52: identification, nomenclature, functional characterization and genetic diseases of RFVT/SLC52. Mol Aspects Med 34, 693–701.